J Electr Eng Technol.2018; 13(6): 2187-2195
http://doi.org/10.5370/JEET.2018.13.6.2187
ISSN(Print) 1975-0102
ISSN(Online) 2093-7423

Nonlinear Excitation Control Design of Generator Based on Multi-objective Feedback

Dengyi Chen†, Xiaocong Li* and Song Liu*

Abstract – In order to realize the multi-objective control of single-input multi-output nonlinear differential algebraic system (NDAS) and to improve the dynamic characteristics and static accuracy, a design method of nonlinear control with multi-objective feedback (NCMOF) is proposed, the principium of this method to arrange system poles, as well as its nature to coordinate dynamic characteristics and static accuracy of the system are analyzed in detail. Through NCMOF design method, the multi-objective control of the system is transformed into linear space, and then it is effectively controlled under the nonlinear feedback control law, the problem to balance all control objectives caused by less input and more output of the system thus is solved. Applying NCMOF design method to generator excitation system, the nonlinear excitation control law with terminal voltage, active power and rotor speed as objective outputs is designed. Simulation results show that NCMOF can not only improve the dynamic characteristics of generator, but also damp the mechanical oscillation of a generator in transient process. Moreover, NCMOF can control the terminal voltage of the generator to the setting value with no static error under typical disturbances.

Keywords: Nonlinear differential algebraic system, Multi-objective feedback, Pole assignment, Excitation control.

1. Introduction

Nonlinear differential algebraic system (NDAS) is a kind of more universal system model, which is widely existed in complex systems such as power system, robot system and restricted mechanical system. For a long time, the research of nonlinear differential algebra system has been paid great attention by scholars [1-4] in the field of power system control. Based on NDAS model, the *M* derivative is defined and the generator excitation controller is designed [3]. However, this controller can not coordinate the dynamic characteristics and static accuracy of the system well.

In the fields of improving transient stability of power system and damping low-frequency oscillation of the system, generator excitation control has been playing a very important role [5, 6]. Therefore, many scholars have conducted in-depth researches on generator excitation control, and a series of control methods such as proportion integral derivative (PID) control method, linear optimal control, backstepping control method [7-9], immersion and invariance control method [10], Hamiltonian control method [1, 4, 11, 12], nonlinear excitation control [13], direct feedback linearization control method [14, 15], differential geometric control method [16] have been accordingly proposed. These methods, especially the non-linear control methods, have greatly improved the system performance. However, some methods select output function as a single state variable in order to achieve a completely accurate linearization of the system, resulting in a static offset [3, 16] of the generator terminal voltage. Partial accurate linearization proposed in [5] suggested an effective approach to solve the problem. The partial accurate linearization [5, 17, 18] selects a number of state variables as the output function to realize non-deviation adjustment of the terminal voltage, which can effectively coordinate the dynamic and static performances of the system. However, this method requires that the input and output dimensions of the system have to be equal. For soluting this problem, researchers [19] proposes the objective holographic feedback method, which achieves low-dimensional input control of high-dimensional output while taking into account the dynamic and static performances of the generator. However, this method is still not involved in the study of differential algebra system.

In order to realize the multi-objective control of nonlinear differential algebraic system and to improve the dynamic characteristics and static accuracy of the system, NCMOF design method is proposed and deeply studied in this paper based on SIMO nonlinear differential algebraic system model. NCMOF has flexibly overcome the difficulty in control law designing caused by implicit function included in the NDAS. In the design process, there is no need to solve the cumbersome Lie derivative [5] or *M* derivative [3], nor is it necessary to prove the complex zero dynamic stability. In this paper, we first designed the NCMOF

† Corresponding Author: College of Electrical Engineering, Guangxi University, China. (125522477@qq.com)
* College of Electrical Engineering, Guangxi University, China. (lhtlht@gxu.edu.cn, songliu_gxu@163.com)
Received: December 21, 2017; Accepted: June 20, 2018

feedback control law in an approximate linear system of NDAS by using the Hartman-Grobman theory [18]. On basis of this work, the essential relation between it and the linear system as well as its effective working mechanism were deeply studied and consequently deduced. At last it was proved that NCMOF corrects the feedback coefficient of the nonlinear feedback law with objective variable, such that adjusts the neighbouring characteristic root of the system equilibrium point to achieve satisfactory dynamic and static-state performance, which ensures accurate tracking of the objective variable. Applying NCMOF to generator excitation system, the simulation results showed that NCMOF can improve the transient stability and static accuracy of the system with satisfactory performance.

2. NCMOF Design Principle

2.1 NCMOF design method

Considering the following SIMO nonlinear differential algebraic system:

$$\begin{cases} \dot{\boldsymbol{x}} = \boldsymbol{f}(\boldsymbol{x},\boldsymbol{w}) + \boldsymbol{g}(\boldsymbol{x},\boldsymbol{w})u \\ \boldsymbol{0} = \boldsymbol{\rho}(\boldsymbol{x},\boldsymbol{w}) \\ \boldsymbol{y} = \boldsymbol{h}(\boldsymbol{x},\boldsymbol{w}) \end{cases} \tag{1}$$

where $\boldsymbol{x} \in R^n$ and $\boldsymbol{w} \in R^l$ respectively represents the state vector and constraint vector of the system. $u \in R$ represents the control scalar, $\boldsymbol{y} \in R^m$ the output function scalar, while $\boldsymbol{f}$, $\boldsymbol{g}$: $R^n \times R^l \to R^n$ and $\boldsymbol{\rho}: R^n \times R^l \to R^l$ are smooth vector fields that are different for both $\boldsymbol{x}$ and $\boldsymbol{w}$. $\boldsymbol{h}$: $R^n \times R^l \to R^m$. n, l and m are all positive integers. The difference between the system and traditional affine nonlinear system is that implicit function algebraic equation $\boldsymbol{0}=\boldsymbol{\rho}(\boldsymbol{x},\boldsymbol{w})$ is more, it is difficult to solve the explicit function form of $\boldsymbol{w}$ concerning $\boldsymbol{x}$: $\boldsymbol{w}=\boldsymbol{F}(\boldsymbol{x})$. In this way, it is impossible to work out the *Lie* derivative $L_f h_m(\boldsymbol{x})$ or *M* derivative of the objective output $h_m(\boldsymbol{x})$, so it is difficult to obtain the feedback control law u of the original system.

Assuming $\boldsymbol{y}_r = [y_{1r}, \cdots, y_{mr}]^T$ is the set point that the output function $\boldsymbol{y}$ wishing to track, then the tracking deviation of the objective output can be represented as

$$I_i = y_i - y_{ir} \quad (i = 1, \cdots, m) \tag{2}$$

where I_i is the tracking deviation of the output variable $\boldsymbol{y}_i$.

Remark 1: The design objective of nonlinear differential algebraic control system is mainly to realize that when the system (1) is disturbed, the designed nonlinear feedback law can make the system transiently stable and ensure the tracking deviation of objective output converging quickly to zero, that is

$$\lim_{t\to\infty} |I_i| = 0 \quad (i = 1, \cdots, m) \tag{3}$$

Thus, the tracking deviation of the objective output converging to zero means that the static accuracy of controlled system is solved.

Assume that there is an element y_m in objective output vector $\boldsymbol{y}$, the derivation of y_m directly satisfies

$$\dot{y}_m = \boldsymbol{L}_1(\boldsymbol{x},\boldsymbol{w},\dot{\boldsymbol{w}}) + \boldsymbol{L}_2(\boldsymbol{x},\boldsymbol{w},\dot{\boldsymbol{w}})u \tag{4}$$

where $\boldsymbol{L}_1(\boldsymbol{x},\boldsymbol{w},\dot{\boldsymbol{w}})$ and $\boldsymbol{L}_2(\boldsymbol{x},\boldsymbol{w},\dot{\boldsymbol{w}})$ are respectively the functions of $\boldsymbol{x},\boldsymbol{w},\dot{\boldsymbol{w}}$, and $\boldsymbol{L}_2(\boldsymbol{x},\boldsymbol{w},\dot{\boldsymbol{w}}) \neq 0$.

Dynamic equation is actively set up by the tracking deviation in Eq. (2), to satisfy the Brunovsky normal form

$$\dot{\boldsymbol{I}} = \boldsymbol{A}\boldsymbol{I} + \boldsymbol{b}v \tag{5}$$

Where

$$\boldsymbol{I} = \begin{bmatrix} I_1 \\ I_2 \\ \vdots \\ I_{m-1} \\ I_m \end{bmatrix} = \begin{bmatrix} y_1 - y_{1r} \\ y_2 - y_{2r} \\ \vdots \\ y_{m-1} - y_{(m-1)r} \\ y_m - y_{mr} \end{bmatrix}, \quad \boldsymbol{A} = \begin{bmatrix} 0 & 1 & 0 & \cdots & 0 \\ 0 & 0 & 1 & \cdots & 0 \\ \vdots & \vdots & \vdots & \vdots & \vdots \\ 0 & 0 & 0 & \cdots & 1 \\ 0 & 0 & 0 & \cdots & 0 \end{bmatrix}$$

$$\boldsymbol{b} = \begin{bmatrix} 0 & 0 & 0 & \cdots & 1 \end{bmatrix}^T$$

In Eq. (5),

$$v = \dot{y}_m - \dot{y}_{mr} = \boldsymbol{L}_1(\boldsymbol{x},\boldsymbol{w},\dot{\boldsymbol{w}}) + \boldsymbol{L}_2(\boldsymbol{x},\boldsymbol{w},\dot{\boldsymbol{w}})u - \dot{y}_{mr} \tag{6}$$

the linear feedback control law of system (5) is obtained by linear optimal theory

$$v = -k_1 I_1 - k_2 I_2 - \cdots - k_m I_m \tag{7}$$

Combining Eq. (6) and (7), the multi-objective feedback nonlinear control law u of the SIMO nonlinear differential algebraic system (1) can be represented as

$$u = [-k_1 I_1 - k_2 I_2 - \cdots - k_m I_m - \boldsymbol{L}_1(\boldsymbol{x},\boldsymbol{w},\dot{\boldsymbol{w}}) + \dot{y}_{mr}] / \boldsymbol{L}_2(\boldsymbol{x},\boldsymbol{w},\dot{\boldsymbol{w}}) \tag{8}$$

Observing Eq. (8) it can be seen that appropriate selection of $\boldsymbol{L}_1(\boldsymbol{x},\boldsymbol{w},\dot{\boldsymbol{w}})$ and $\boldsymbol{L}_2(\boldsymbol{x},\boldsymbol{w},\dot{\boldsymbol{w}})$ can achieve control law design based on local information. When the system (5) is disturbed, NCMOF control law (8) makes the system steady, then $(y_i - y_{ir})' = \dot{y}_i - \dot{y}_{ir} = 0$, that is, dynamic characteristic of the objective output of the system (1) is effectively constrained and maintaining stable. In addition, from Eq. (5) we can get $(y_i - y_{ir})' = y_{i+1} - y_{(i+1)r} = 0$, which indicates that the error between objective output and its reference value eventually converges to zero. Thus it can be seen that NCMOF takes full account of stability of the transient process when the system is disturbed, and it also ensures static accuracy of the system after stabilization, so that the performance of the two indicators achieve a reasonable fit.

Remark 2: It can be seen from the Eqs. (2) and (7) that

NCMOF transforms and combines objective output in the nonlinear system (1) into the linear system (5), feedback is achieved via nonlinear control law, and the dynamic and static performance of the objective output is constrained, correspondingly dynamic and static-state performance of the system is coordinated. NCMOF does not require input control variable exactly equal to output objective variable, and in fact, NCMOF is still able to achieve effective feedback control of multiple objectives when the control variable is much less than the objective variable. There is also no need to solve complex Lie derivative or M derivative in the whole design process, which has great flexibility and extensive engineering practicality.

2.2 Pole assignment principle of NCMOF

Hartman-Grobman theorem indicates that: In the neighborhood of hyperbolic singular point of nonlinear system, the nonlinear system topology is equivalent to its primary approximation system.

Remark 3: In this paper, the principle and essence of NCMOF design method in the effective operation of SIMO nonlinear differential algebraic system are deeply studied by using the Hartmann-Grobman theorem, the fundamental causes of NCMOF to improve dynamic characteristics of the system and to achieve static zero deviation of objective output, as well as the ability of NCMOF to coordinate dynamic and static-state performance of system are revealed.

When the system (1) expands Taylor series at the equilibrium point x_e, the primary approximation system can be represented as

$$\begin{cases} \dot{\boldsymbol{x}} = \boldsymbol{Ax} + \boldsymbol{Cw} + \boldsymbol{b}u \\ \boldsymbol{0} = \boldsymbol{Ex} + \boldsymbol{Fw} \\ \boldsymbol{y} = \boldsymbol{Dx} + \boldsymbol{Gw} \end{cases} \tag{9}$$

where $\boldsymbol{A} \in R^{n\times n}$, $\boldsymbol{C} \in R^{n\times l}$, $\boldsymbol{E} \in R^{l\times n}$, $\boldsymbol{F} \in R^{l\times l}$, $\boldsymbol{D} \in R^{m\times n}$, $\boldsymbol{G} \in R^{m\times l}$ are constant matrixes, and $\boldsymbol{b} \in R^{n}$ is a constant column vector.

Substituting $\boldsymbol{w} = -\boldsymbol{F}^{-1}\boldsymbol{Ex}$ to Eq. (9) and simplifying to the following linear system:

$$\begin{cases} \dot{\boldsymbol{x}} = \boldsymbol{A'x} + \boldsymbol{b}u \\ \boldsymbol{y} = \boldsymbol{C'x} \end{cases} \tag{10}$$

where

$$\boldsymbol{A}' = \boldsymbol{A} - \boldsymbol{CF}^{-1}\boldsymbol{E},\ \boldsymbol{C}' = \boldsymbol{D} - \boldsymbol{GF}^{-1}\boldsymbol{E}$$

Selecting the nonsingular matrix $\boldsymbol{T}_c$ and linearly transforming the Eq. (10) to $\boldsymbol{x}_c=\boldsymbol{T}_c\boldsymbol{x}$, after further simplification controllable normal linear system can be obtained

$$\begin{cases} \dot{\boldsymbol{x}}_c = \boldsymbol{A}_c\boldsymbol{x}_c + \boldsymbol{b}_c u \\ \boldsymbol{y}_c = \boldsymbol{C}_c\boldsymbol{x}_c \end{cases} \tag{11}$$

where

$$\boldsymbol{C}_c = \boldsymbol{C}'\boldsymbol{T}_c^{-1} = \begin{bmatrix} \boldsymbol{C}_{c1} \\ \vdots \\ \boldsymbol{C}_{cm} \end{bmatrix},\ \boldsymbol{C}_{ci} = \begin{bmatrix} c_{i1} & \cdots & c_{in} \end{bmatrix},$$

$$\boldsymbol{A}_c = \begin{bmatrix} 0 & 1 & 0 & \cdots & 0 \\ 0 & 0 & 1 & \cdots & 0 \\ \vdots & \vdots & \vdots & \vdots & \vdots \\ 0 & 0 & 0 & \cdots & 1 \\ -a_0 & -a_1 & -a_2 & \cdots & -a_{n-1} \end{bmatrix},\ \boldsymbol{b}_c = \begin{bmatrix} 0 \\ 0 \\ \vdots \\ 0 \\ 1 \end{bmatrix}$$

Assume that there is a reference state $\boldsymbol{x}_{cr}$, a reference output $\boldsymbol{y}_{cr}$ and a reference input u_r, satisfying the system (11), that is

$$\begin{cases} \dot{\boldsymbol{x}}_{cr} = \boldsymbol{A}_c\boldsymbol{x}_{cr} + \boldsymbol{b}_c u_r \\ \boldsymbol{y}_{cr} = \boldsymbol{C}_c\boldsymbol{x}_{cr} \end{cases} \tag{12}$$

Based on Eq. (4), it is known that the system (11) exists

$$\dot{y}_{cm} = (\boldsymbol{C}_{cm}^1 + \boldsymbol{C}_{cm}^2)\dot{\boldsymbol{x}}_c = \boldsymbol{C}_{cm}^1\dot{x}_c + \boldsymbol{C}_{cm}^2\dot{\boldsymbol{x}}_c \tag{13}$$

where

$$\boldsymbol{C}_{cm}^1 = \begin{bmatrix} c_{m1}^1 & \cdots & c_{mn}^1 \end{bmatrix},\ \boldsymbol{C}_{cm}^2 = \begin{bmatrix} c_{m1}^2 & \cdots & c_{mn}^2 \end{bmatrix}$$

Eq. (13) can be resolved into

$$\dot{y}_{cm} = \boldsymbol{C}_{cm}^1\dot{\boldsymbol{x}}_c + \boldsymbol{C}_{cm}^2(\boldsymbol{A}_c\boldsymbol{x}_c + \boldsymbol{b}_c u) \tag{14}$$

Obviously, the reference output y_{cmr} of y_{cm} in Eq. (12) also exists

$$\dot{y}_{cmr} = \boldsymbol{C}_{cm}^1\dot{\boldsymbol{x}}_{cr} + \boldsymbol{C}_{cm}^2(\boldsymbol{A}_c\boldsymbol{x}_{cr} + \boldsymbol{b}_c u) \tag{15}$$

Combining Eq. (11) and (12) obtains

$$\begin{cases} \Delta\dot{\boldsymbol{x}}_c = \boldsymbol{A}_c\Delta\boldsymbol{x}_c + \boldsymbol{b}_c\Delta u \\ \Delta\boldsymbol{y}_c = \boldsymbol{C}_c\Delta\boldsymbol{x}_c \end{cases} \tag{16}$$

where

$$\Delta\boldsymbol{x}_c = \boldsymbol{x}_c - \boldsymbol{x}_{cr}, \Delta u_c = u_c - u_{cr}, \Delta\boldsymbol{y}_c = \boldsymbol{y}_c - \boldsymbol{y}_{cr}$$

Combining Eq. (14) and (15), we get

$$\Delta\dot{y}_{cm} = \boldsymbol{C}_{cm}^1\Delta\dot{\boldsymbol{x}}_c + \boldsymbol{C}_{cm}^2(\boldsymbol{A}_c\Delta\boldsymbol{x}_c + \boldsymbol{b}_c\Delta u) \tag{17}$$

where

$$\Delta y_{cm} = y_{cm} - y_{cmr}$$

According to the proposed NCMOF design method, and with reference to Eq. (8), feedback control law of the linear control system (11) can be obtained by simplifying Eq. (17)

$$\Delta u = (\boldsymbol{C}_{cm}^2 \boldsymbol{b}_c)^{-1}(V_c - \boldsymbol{C}_{cm}^2 \boldsymbol{A}_c \Delta \boldsymbol{x}_c - \boldsymbol{C}_{cm}^1 \Delta \dot{\boldsymbol{x}}_c) \quad (18)$$

where

$$V_c = -k_{c1}(y_{c1} - y_{c1r}) - \cdots - k_{cm}(y_{cm} - y_{cmr})$$

Substituting Eq. (18) into (16) obtains

$$\begin{aligned}\Delta \dot{\boldsymbol{x}}_c = \boldsymbol{A}_c \Delta \boldsymbol{x}_c + \boldsymbol{b}_c[(\boldsymbol{C}_{cm}^2 \boldsymbol{b}_c)^{-1} \\ (V_c - \boldsymbol{C}_{cm}^2 \boldsymbol{A}_c \Delta \boldsymbol{x}_c - \boldsymbol{C}_{cm}^1 \Delta \dot{\boldsymbol{x}}_c)]\end{aligned} \quad (19)$$

Let $\boldsymbol{K}_c = [-k_{c1} \ \cdots \ -k_{cm}]$
it can be obtained by finishing Eq. (19)

$$\begin{aligned}&[\boldsymbol{I} + \boldsymbol{b}_c(\boldsymbol{C}_{cm}^2 \boldsymbol{b}_c)^{-1} \boldsymbol{C}_{cm}^1] \Delta \dot{\boldsymbol{x}}_c \\ &= [\boldsymbol{A}_c + \boldsymbol{b}_c(\boldsymbol{C}_{cm}^2 \boldsymbol{b}_c)^{-1}(\boldsymbol{K}_c \boldsymbol{C}_c - \boldsymbol{C}_{cm}^2 \boldsymbol{A}_c)] \Delta \boldsymbol{x}_c\end{aligned} \quad (20)$$

after further finishing it can be obtained

$$\Delta \dot{\boldsymbol{x}}_c = \overline{\boldsymbol{A}}_c \Delta \boldsymbol{x}_c \quad (21)$$

where

$$\overline{\boldsymbol{A}}_c = \begin{bmatrix} 0 & 1 & 0 & \cdots & 0 \\ 0 & 0 & 1 & \cdots & 0 \\ \vdots & \vdots & \vdots & \vdots & \vdots \\ 0 & 0 & 0 & \cdots & 1 \\ -\overline{k}_{c0} & -\overline{k}_{c1} & -\overline{k}_{c2} & \cdots & -\overline{k}_{c(n-1)} \end{bmatrix},$$

$$\overline{k}_{c0} = \frac{c_{11}k_{c1} + \cdots + c_{m1}k_{cm}}{c_{mn}^2},$$

$$\overline{k}_{ci} = \frac{c_{1(i+1)}k_{c1} + \cdots + c_{m(i+1)}k_{cm} + c_{mi}}{c_{mn}^2}, \ (i = 1, \cdots, n-1)$$

Thus, the characteristic polynomial of Eq. (21) is

$$\boldsymbol{f}(\lambda) = \lambda^n + \overline{k}_{c(n-1)}\lambda^{n-1} + \cdots + \overline{k}_{c1}\lambda + \overline{k}_{c0} \quad (22)$$

Remark 4: In observation of Eq. (22), it can be seen that the pole of Eq. (16) can be arranged at a suitable position by selecting appropriate feedback coefficient $\boldsymbol{K}_c$ and $\boldsymbol{C}_{cm}^1$, that is, eigenvalues of the closed-loop system (9) are arbitrarily arranged. As long as eigenvalues are negative real roots, the original closed-loop system is stable according to the Hartman-Grobman theorem, hence no proof of zero dynamic stability is needed during the design process. It also can be seen that the feedback coefficient in nonlinear feedback law has a significant effect on performance of objective output of the system. Selecting appropriate feedback coefficient can make the dynamic response of objective output more quickly and steadily, and also the static tracking more accurate after stabilization.

3. Design of Generator Excitation Control Law for Differential Algebraic Model

3.1 System state equation

The paper applies NCMOF to single machine infinite bus power system as shown below in Fig. 1 to study the generator control problem.

Generator state equation of single-machine infinite system is

$$\begin{cases} \dot{\delta} = (\omega - 1)\omega_0 \\ \dot{\omega} = [P_m - P_e - D(\omega - 1)]/T_J \\ \dot{E}'_q = (E_f - E_q)/T'_{d0} \end{cases} \quad (23)$$

In Eq. (23), the relation (differential algebraic equation) between constraint variable $w = [E_q \ U_t \ P_e]^T$ and state variable $x = [\delta \ \omega \ E'_q]^T$ is as follows:

$$P_e = E'_q I_q \quad (24)$$

$$E_q = E'_q + (x_d - x'_d)I_d \quad (25)$$

$$U_{tq} = E'_q - x'_d I_d \quad (26)$$

$$U_{td} = x_q I_q \quad (27)$$

$$U_t = \sqrt{U_{td}^2 + U_{tq}^2} \quad (28)$$

where δ is the rotor angle of generator, ω is the rotor speed, E'_q is the transient EMF in the q-axis, and E_q is the EMF in the q-axis. P_m and P_e are the mechanical power input and the active power. T'_{d0} is the time constant of excitation winding, T_J, D and ω_0 denote the inertia coefficient, damping constant and synchronous machine speed of the rotor respectively. U_t, U_{td} and U_{tq} are respectively the generator terminal voltage, d-axis terminal voltage and q-axis terminal voltage. E_f is the controlled variable, denoting the excitation voltage. I_d and I_q are the d-axis currents and q-axis currents of the stator. x_d, x'_d and x_q denote the d-axis reactance, d-axis transient reactance and q-axis reactance, respectively. In the equation, the unit of δ is radian (rad), the unit of time constant is second (s), while the others is *pu*.

Finishing Eq. (23) to (28), the third-order generator excitation system model is transformed into normal SIMO nonlinear differential algebraic system, that is

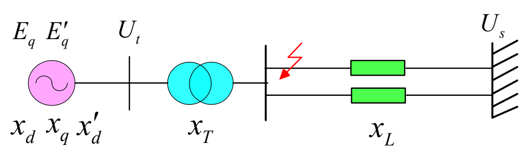

Fig. 1. Single machine infinite bus power system

$$\begin{cases} \dot{\boldsymbol{x}} = \boldsymbol{f}(\boldsymbol{x},\boldsymbol{w}) + \boldsymbol{g}(\boldsymbol{x},\boldsymbol{w})\boldsymbol{u} \\ \boldsymbol{0} = \boldsymbol{\rho}(\boldsymbol{x},\boldsymbol{w}) \\ \boldsymbol{y} = \boldsymbol{h}(\boldsymbol{x},\boldsymbol{w}) \end{cases} \tag{29}$$

where

$$\boldsymbol{f}(\boldsymbol{x},\boldsymbol{w}) = \begin{bmatrix} (\omega-1)\omega_0 \\ [P_m - P_e - D(\omega-1)]/T_J \\ -E_q/T'_{d0} \end{bmatrix},$$

$$\boldsymbol{g}(\boldsymbol{x},\boldsymbol{w}) = [0\ 0\ 1/T'_{d0}]^T,$$

$$\boldsymbol{\rho}(\boldsymbol{x},\boldsymbol{w}) = \begin{bmatrix} P_e - E'_q I_q \\ E_q - E'_q - (x_d - x'_d)I_d \\ U_t - \sqrt{(E'_q - x'_d I_d)^2 + (x'_d I_q)^2} \end{bmatrix}$$

3.2 NCMOF Control Law Design

For generator, the engineering practice is mainly concerned with whether terminal voltage U_t, speed ω and output active power P_e these three variables can accurately track their set points within allowable ranges. In fact, the set points of these three physical variables are specified by power dispatch department, thus the tracking objectives of these three physical variables can be obtained:

$$\begin{cases} P_{er} = P_0 \\ \omega_r = 1 \\ U_{tr} = U_0 \end{cases} \tag{30}$$

where U_0, *1* and P_0 are respectively the set points of generator terminal voltage, angular frequency and electromagnetic active power.

Therefore, the objective output tracking deviation equation of generator can be written as

$$\begin{cases} I_1 = P_e - P_0 \\ I_2 = \omega - 1 \\ I_3 = U_t - U_0 \end{cases} \tag{31}$$

Based on NCMOF design method and Eq. (31), the equation that conforms to Brunovsky normal form can be obtained:

$$\begin{bmatrix} (P_e - P_{e0})' \\ (\omega-1)' \\ (U_t - U_{t0})' \end{bmatrix} = \begin{bmatrix} 0 & 1 & 0 \\ 0 & 0 & 1 \\ 0 & 0 & 0 \end{bmatrix} \begin{bmatrix} P_e - P_{e0} \\ \omega - 1 \\ U_t - U_{t0} \end{bmatrix} + \begin{bmatrix} 0 \\ 0 \\ 1 \end{bmatrix} v \tag{32}$$

Through the linear optimal control theory we get

$$v = -k_1(P_e - P_0) - k_2(\omega-1) - k_3(U_t - U_{t0}) \tag{33}$$

Combining Eq. (25), (26) and (27), the derivative of U_t can be obtained as follows:

$$\dot{U}_t = D_1 + D_2 E_f \tag{34}$$

where

$$\begin{cases} D_1 = \dfrac{1}{U_t}\Big[x'^2_d I_q \dot{I}_q - \dfrac{1}{T'_{d0}}\sqrt{U_t^2 - (x'_d I_q)^2}\cdot \\ \quad (\sqrt{U_t^2 - (x'_d I_q)^2} + x_d I_d + T'_{d0} x'_d \dot{I}_d)\Big] \\ D_2 = \sqrt{U_t^2 - (x'_d I_q)^2}\Big/(U_t T'_{d0}) \end{cases} \tag{35}$$

in the equation, differentials of I_d and I_q will weaken robustness of the control law, where these two variables are ignored, Eq. (35) can be written as

$$\begin{cases} D_1 \approx \dfrac{1}{U_t}\Big[- \dfrac{1}{T'_{d0}}\sqrt{U_t^2 - (x'_d I_q)^2}\cdot \\ \quad (\sqrt{U_t^2 - (x'_d I_q)^2} + x_d I_d)\Big] \\ D_2 = \sqrt{U_t^2 - (x'_d I_q)^2}\Big/(U_t T'_{d0}) \end{cases} \tag{36}$$

According to the principle of NCMOF, substituting Eq. (33) and (34) to (32) and simplifying, the multi-objective feedback nonlinear excitation control law of the system (20) is

$$\begin{aligned} E_f &= (v - D_1)/D_2 \\ &= [-k_1(P_e - P_0) - k_2(\omega-1) - \\ &\quad k_3(U_t - U_{t0}) - D_1]/D_2 \end{aligned} \tag{37}$$

here the mapping from v to E_f is reversible as $D_2 \neq 0$.

Remark 5: In observation of Eq. (37), it can be found that I_q and I_d are difficult to measure in engineering practice. In this paper, these two virtual physical variables are mathematically deduced further, and the equivalent actual physical variables which easy to measure are found out to facilitate the engineering realization of control laws.

Virtual voltage is introduced

$$E_Q = U_{tq} + I_d x_q \tag{38}$$

where

$$\Delta U_2 = \frac{Q_e x_q}{U_t},\quad \delta U_2 = \frac{P_e x_q}{U_t}$$

it can be seen from the principle of network voltage dropping in power system

$$E_Q = \sqrt{(U_t + \Delta U_2)^2 + (\delta U_2)^2} \tag{39}$$

synchronous generator reactive power output is

$$Q_e = U_{tq} I_d - U_{td} I_q \tag{40}$$

Combining Eq. (26), (27), (28) and (40), it can be further consolidated as follows:

$$I_d = \frac{(Q_e + x_q I^2)}{E_Q} \tag{41}$$

consolidating Eq. (41), the q-axis current can be represented as

$$I_q = \sqrt{I^2 - I_d^{\,2}} \tag{42}$$

4. Simulation Verification

4.1 Simulation system

The simulation parameters of generator are as follows: x_d=2.12, x_q=2.12, $x'_d = 0.26$, $x_T = 0.106$, D=2, $T_J = 4.06$, $T'_{d0} = 5.8$. The initial working points are: P_0=0.6 pu, δ_0=50°, V_0=1.02926 pu. To illustrate the correctness and superiority of NCMOF control method, it was compared with the state feedback exact linearization (SFEL) [15] method which with y=Δδ as output function, the simulation comparison was done in the aspects of dynamic and static-state performance. In addition, automatic voltage regulator (AVR)+power system stabilizers (PSS) is also chosen as a comparison. In the simulation diagram, solid line represents NCMOF, dotted line indicates SFEL and dashed line denotes AVR+PSS.

The model of AVR+PSS is shown in Fig. 2, and its parameter is as follows [20]:

$K_A = 195$, $T_R = 0.016s$, $E_{f\max} = 7.0$, $E_{f\min} = -7.0$, $K_{PSS} = 21$, $T_W = 10s$, $T_1 = 0.045s$ $T_2 = 0.025s$, $T_3 = 3.0s$, $T_4 = 5.4s$, $v_{s\min} = -0.2$ $v_{s\max} = 0.2$.

4.2 System pole assignment

In Eq. (38), if k_1=42.6, k_2=-3ω_0 and k_3=34.8 were selected, the pole of closed-loop system (29) at equilibrium point can be arranged at the following position under NCMOF: $s_1 = -161.51$, $s_2 = -2.78$+j2.36 , $s_3 = -2.78$+j2.36 . All poles are located in the left half of the complex plane,

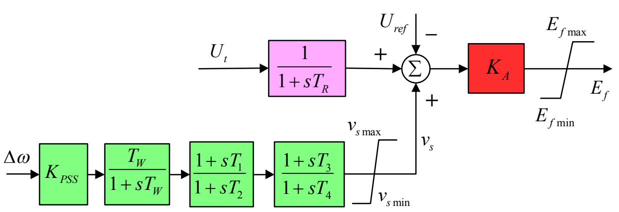

Fig. 2. The PSS+AVR controller

and the system (29) is asymptotically stable by the Lyapunov theorem.

4.3 Simulation results analysis

4.3.1 Input power adjustment disturbance

This simulation means that when t=0.5s, the input mechanical power P_m of generator suddenly increased by 10% from 0.6 to 0.7--the purpose is to observe the tracking performance of generator after sudden change of the input mechanical power, and see whether there is a static error. The simulation curve of generator is shown in Fig. 3.

It can be seen from Fig. 3(a) that the control of NCMOF makes generator terminal voltage to track its set point quickly with no static difference, in contrast, SFEL produces a static offset of 4%. Fig. 3(b) shows that NCMOF，SFEL and AVR+PSS all can ensure generator a good power tracking characteristic. From Fig. 3(c) and (d) it can be seen that NCMOF, SFEL, AVR+PSS can quickly and smoothly transit the rotor angle and the speed of generator to a stable state. Fig. 3(d) indicates that NCMOF and AVR+PSS achieve an increase in active power by increasing rotor angle, while SFEL takes stabilizing rotor angle at initial operating point as the objective. Therefore, to meet the increasing demand of electromagnetic power, the excitation voltage can be only increased, which resulting in generator terminal voltage deviation from the standard value, and consequently causing static offset.

Fig. 3 indicates that NCMOF control law realized accurate tracking of active power under the condition of ensuring terminal voltage no static difference, and its control effect is better compared with that of the exact linearization method. AVR+PSS can also achieve this effect, but the oscillation in transient process is larger than NCMOF.

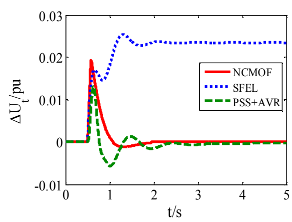

(a) The curve of ΔU_t

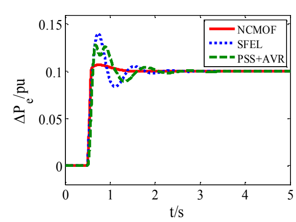

(b) The curve of ΔP_e

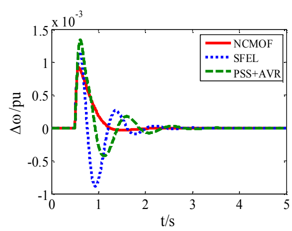

(c) The curve of $\Delta\omega$

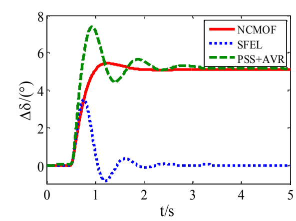

(d) The curve of $\Delta\delta$

Fig. 3. Response curve of generator under power disturbance

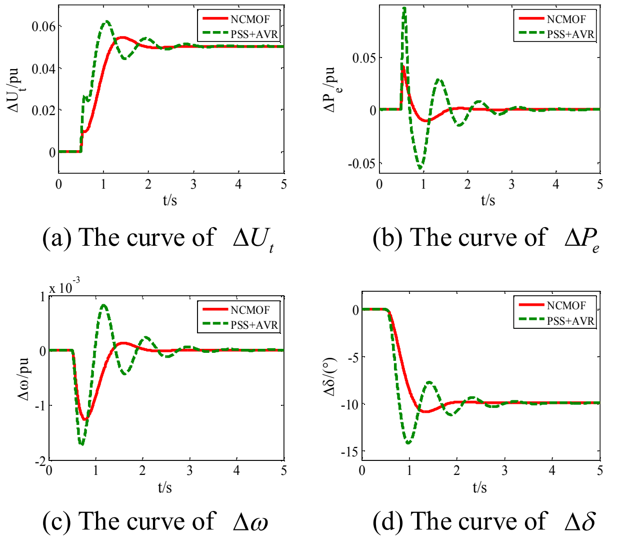

(a) The curve of ΔU_t (b) The curve of ΔP_e

(c) The curve of $\Delta\omega$ (d) The curve of $\Delta\delta$

Fig. 4. Response curve of generator under disturbance of voltage regulation

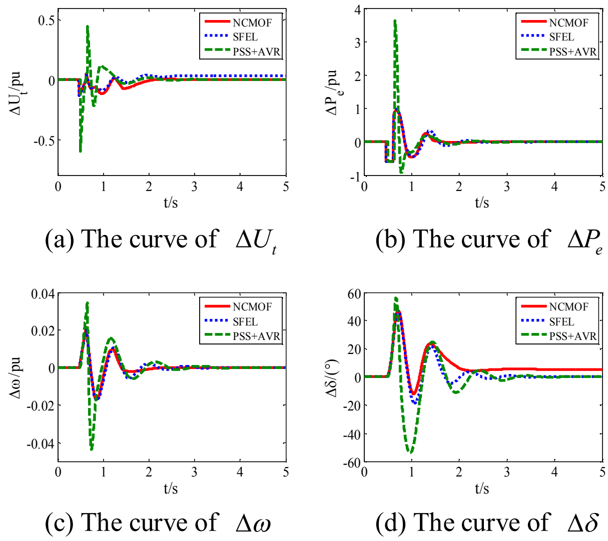

(a) The curve of ΔU_t (b) The curve of ΔP_e

(c) The curve of $\Delta\omega$ (d) The curve of $\Delta\delta$

Fig. 5. Response curve of generator under short-circuit disturbance

4.3.2 Voltage adjustment disturbance

In order to examine the tracking ability of generator to the voltage reference, the voltage set point is suddenly increased by 5% during the simulation. SFEL does not take the role of generator terminal voltage into account, thus it can not be compared with NCMOF in this simulation. From Fig. 4 (a) it can be seen that NCMOF makes generator quickly tracking its voltage reference value, what's more, the deviation between terminal voltage and set point converges to zero after the stabilization of disturbance, with no static error, however, the transient adjustment process of AVR+ PSS is longer. Fig.4 (c) and (d) indicate that NCMOF can well damp the mechanical oscillation of generator, and its overshoot in adjustment process is also small, while the mechanical oscillation of the generator is strong under the control of PSS+AVR

4.3.3 Three-phase Short-circuit Disturbance

This simulation means that when t=0.5s, three-phase short-circuit fault occurred at high-voltage side of the step-up transformer lasts 0.15s--the purpose is to assess the transient adjustment ability of generator under large disturbance, and to find the static tracking error of each state after stabilization of the system. The relevant simulation curve of generator is shown in Fig. 5. Fig. 5(a) indicates that NCMOF can guarantee generator terminal voltage running on the reference voltage after short circuit fault, accurate tracking with no deviation can be realized, while the SFEL causes generator terminal voltage deviation from the pre-fault state. This is because the NCMOF control law effectively constraints and controls the generator terminal voltage. But, it can be seen from the Fig. 5(d), SFEL only requires the rotor angle maintaining constant after the fault, it has no performance requirement for the terminal voltage. Therefore, from Fig. 5 we can see NCMOF effectively damps the frequency oscillation and improves the transient stability of generator, it ensures each concerned variable of generator a good output characteristic. Comparatively, the voltage and frequency based AVR+PSS control show worse dynamics of bigger overshoots and longer settling times as the stronger oscillations of rotor angle and active power.

5. Conclusion

In view of objective output more than input control, NCMOF maps multiple objective outputs that engineering actually concerned to the linear system and restrains them in the nonlinear feedback control law, accordingly it realizes precise and stable tracking of multiple objective outputs. The essence of NCMOF nonlinear design is revealed in this paper, i.e. reasonable selection of nonlinear feedback coefficient can effectively arrange the pole of closed-loop system, which ensures the system a good dynamic and static-state performance. NCMOF design method proposed in this paper has no need to solve the cumbersome Lie derivative or M derivative, nor is it necessary to prove the complex zero dynamic stability, with great flexibility and convenience. The application of NCMOF in single-machine infinite system indicates that this method can improve dynamic characteristics of the generator and guarantee static zero deviation adjustment of the objective output, so it can reasonably coordinate dynamic and static characteristics of the generator. The whole design process is simple and smooth, easy to master. This method can also be used for other similar nonlinear systems, it is believed to have a good application prospect.

Acknowledgments

This research is supported by the National Natural Science Foundation of China (51267001), Guangxi scientific research and technical development project (14122006-29) and Guangxi Natural Science Foundation (2014GXNSFAA118338).

References

[1] L. Li, F. Yu, and X. Liu, "Feedback control of fractional nonlinear differential algebraic systems with Hamiltonian function method," *Appl. Math. Comput.,* vol. 197, no. 2, pp. 904-913, 2008.

[2] Q. Zang, K.F. Zhang, X.Z. Dai et al, "Invertibility of nonlinear differential-algebraic-equation subsystems with application to power systems," *Math. Probl. Eng.,* vol. 2013, pp. 1-8, 2013.

[3] G.H. Xu, J. Wang, and C. Chen, "Feedback stabilization for AC/DC power system with nonlinear loads," *Electr. Pow. Syst. Res*., nov. 74, no. 2, pp. 247-255, Jan. 2005.

[4] B.C. Sung, S.M. Baek, and J.W. Park, "Dynamic embedded optimization applied to power system stabilizers," *J. Electr. Eng. Technol.*, vol. 9, no. 2, pp. 390-398, May 2014.

[5] X.C. Li, M.Y. Chen, Z.J. Liang et al, "Excitation and steam-valving coordinated robust controller design for multi-machine power systems based on the multi-index nonlinear robust control approach," *IEEJ Trans. Electr. Electron. Eng*., vol. 11, no. 4, pp. 425-434, 2016.

[6] F. Liu, R. Yokoyama, Y.C. Zhou et al, "Free-weighting matrices-based robust wide-area FACTS control design with considering signal time delay for stability enhancement of power systems," *IEEJ Trans. Electr. Electron. Eng*., vol. 7, no. 1, pp. 31-39, 2012.

[7] A. Karimi and A. Feliachi, "Decentralized adaptive backstepping control of electric power systems," *Electr. Pow. Syst. Res*., vol. 78, no. 3, pp. 484-493, 2008.

[8] Q. Xie, Z.Z. Han, and H.J. Kang, "Adaptive backstepping control for hybrid excitation synchronous machine with uncertain parameters," *Expert Syst. Appl*., vol. 37, no. 10, pp. 7280-7284, 2010.

[9] R. Huang, J.H. Zhang, and Z.W. Lin, "Decentralized adaptive controller design for large-scale power systems," *Automatica*, vol. 79, pp. 93-100, 2017.

[10] A. Kanchanaharuthai, "Immersion and Invariance-based Non-linear Coordinated Control for Generator Excitation and Static Synchronous Compensator of Power Systems," *Electr. Pow. Compo. Sys*., vol. 42, no. 10, pp. 1004-1015, Jun 2014.

[11] J. Hao, J. Wang, C. Chen et al, "Nonlinear excitation control of multi-machine power systems with structure preserving models based on Hamiltonian system theory," *Electr. Pow. Syst. Res*., vol. 74, no. 3, pp. 401-408, Apr. 2005.

[12] B.J. Lei, S.M. Fei, "A brand new nonlinear robust control design of SSSC for transient stability and damping improvement of multi-machine power systems via pseudo-generalized Hamiltonian theory," *Control Eng. Pract*., vol. 29, pp.1 47-157, May 2014.

[13] X.C. Li, S.J. Cheng, H. Wei et al, "A high performance nonlinear excitation control for generator unit," *Proceedings of the CSEE*, vol. 22, no. 12, pp. 40-45, Dec. 2003.

[14] C. Zhu, R. Wang, and Y. Zhou, "A new nonlinear voltage controller for power systems," *Electrical Power and Energy Systems,* vol. 19, no. 1, pp. 19-27, 1997.

[15] G. Kenné, R. Goma, H. Nkwawo et al, "An improved direct feedback linearization technique for transient stability enhancement and voltage regulation of power generators," *Electrical Power and Energy Systems*, vol. 32, no. 2, pp. 809-816, 2010.

[16] Q. Lu, Y. Sun, Z. Xu et al, "Decentralized nonlinear optimal excitation control," *IEEE Trans. Power Syst*., vol. 11, no. 4, pp. 1957-1962, Nov. 1996.

[17] X.C. Li, Z.B. Xie, Z.J. Liang et al, "Multi-index nonlinear coordinated control of STATCOM and generator excitation differential algebraic system," *Proceedings of the CSEE*, vol. 34, no. 1, pp. 123-129, Jan. 2014.

[18] X.C. Li, S.J. Cheng, H. Wei et al, "Important effection of the output function in SISO nonlinear control system design," *Proceedings of the CSEE*, vol. 24, no. 10, pp. 52-58, Oct. 2004.

[19] H. Liu, Z.C. Hu, and Y.H. Song, "Lyapunov-based decentralized excitation control for global asymptotic stability and voltage regulation of multi-machine power systems," *IEEE Trans. Power Syst*., vol. 27, no. 4, pp. 2262-2270, Nov. 2012.

[20] P. Kundur. "Power system stability and control," New York: *McGraw-Hill*, 1994, pp. 766-770.

Dengyi Chen received the B.S. and M.S. degrees in 2003 and 2008, respectively. Now, he is currently pursuing the Ph.D. degree in the Department of Electrical Engineering, Guangxi University, China. His research interests include power system stability and control.

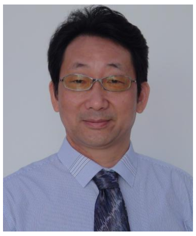

Xiaocong Li received the B.S., M.S., and Ph.D. degrees, all in electrical engineering, in 1982, 1992, and 2004, respectively. Now, he is a Professor and doctoral supervisor in the Department of Electrical Engineering, Guangxi University, China. His research interests include power system analysis and control and power system nonlinear control.

Song Liu received the B.S. degree from China, in electrical engineering. Now, he is currently pursuing the Ph.D. degree in the Department of Electrical Engineering, Guangxi University, China. His research interests include power system stability analysis and nonlinear control, smart grids, and renewable energy.